Ductal Ngn3-expressing progenitors contribute to adult β cell neogenesis in the pancreas

Graphical abstract

Highlights

- Ductal Ngn3+ cells contribute to the beta cell population during homeostasis

- Duct-resident endocrine progenitor cells express somatostatin

- Somatostatin-positive ductal cells are increased in Akita$^{+/-}$ diabetic mice

- scRNA-seq analysis suggests ductal somatostatin+ cells give rise to beta cells
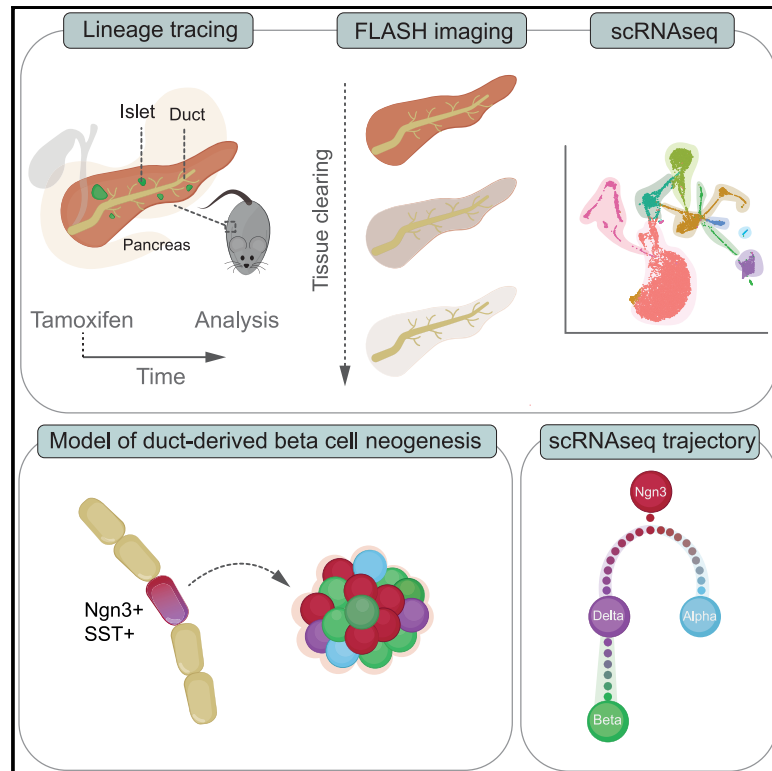
Authors

Christopher Gribben,
Christopher Lambert,
Hendrik A. Messal, ..., Peter Jones,
Rocio Sancho, Axel Behrens

Correspondence

rocio.sancho@kcl.ac.uk (R.S.),
axel.behrens@icr.ac.uk (A.B.)

In brief

A better understanding of adult beta cell neogenesis would open new approaches for diabetes treatment. Gribben et al. used lineage tracing and scRNA-seq to characterize a duct-resident somatostatin-positive endocrine progenitor cell population that is a source of beta cells in homeostasis and during diabetes.

CelPress

Short article

Ductal Ngn3-expressing progenitors contribute to adult β cell neogenesis in the pancreas

Christopher Gribben,[1,9,12] Christopher Lambert,[2,12] Hendrik A. Messal,[1,10] Ella-Louise Hubber,[4] Chloe Rackham,[4,11] Ian Evans,[1] Harry Heimberg,[3] Peter Jones,[4] Rocio Sancho,[2,8,13,*] and Axel Behrens[1,5,6,7,13,14,*]

[1]The Francis Crick Institute, 1 Midland Road, London, UK
[2]Centre for Stem Cells and Regenerative Medicine, King's College London, London, UK
[3]Beta Cell Neogenesis, Vrije Universiteit Brussel, Brussels, Belgium
[4]Department of Diabetes, King's College London, London, UK
[5]Cancer Stem Cell Laboratory, Institute of Cancer Research, London, UK
[6]Division of Cancer, Department of Surgery and Cancer, Imperial College, London, UK
[7]Convergence Science Centre, Imperial College, London SW7 2BU, UK
[8]Department of Internal Medicine III, University Hospital Carl Gustav Carus at the Technische Universität Dresden, Dresden, Germany
[9]Present address: Wellcome Trust-MRC Cambridge Stem Cell Institute, University of Cambridge, Cambridge, UK
[10]Present address: Division of Molecular Pathology, Oncode Institute, the Netherlands Cancer Institute, Amsterdam, the Netherlands
[11]Present address: Exeter Centre for Excellence in Diabetes (EXCEED), Institute of Biomedical & Clinical Science, University of Exeter Medical School, Exeter, UK
[12]These authors contributed equally
[13]Senior author
[14]Lead contact
*Correspondence: rocio.sancho@kcl.ac.uk (R.S.), axel.behrens@icr.ac.uk (A.B.)
https://doi.org/10.1016/j.stem.2021.08.003

SUMMARY

Ductal cells have been proposed as a source of adult β cell neogenesis, but this has remained controversial. By combining lineage tracing, 3D imaging, and single-cell RNA sequencing (scRNA-seq) approaches, we show that ductal cells contribute to the β cell population over time. Lineage tracing using the Neurogenin3 (Ngn3)-CreERT line identified ductal cells expressing the endocrine master transcription factor Ngn3 that were positive for the δ cell marker somatostatin and occasionally co-expressed insulin. The number of hormone-expressing ductal cells was increased in *Akita*^{+/−} diabetic mice, and *ngn3* heterozygosity accelerated diabetes onset. scRNA-seq of Ngn3 lineage-traced islet cells indicated that duct-derived somatostatin-expressing cells, some of which retained expression of ductal markers, gave rise to β cells. This study identified Ngn3-expressing ductal cells as a source of adult β cell neogenesis in homeostasis and diabetes, suggesting that this mechanism, in addition to β cell proliferation, maintains the adult islet β cell population.

INTRODUCTION

The pancreas is central to energy homeostasis, playing essential roles in digestion and in regulation of blood glucose. Glucose homeostasis is controlled by endocrine cells of the islets of Langerhans, which contain mostly insulin-secreting β cells. Type 1 and late-stage type 2 diabetes involve β cell loss (Kharroubi and Darwish, 2015). With 1 in 11 people being diabetic, there is a great need to understand how the adult β cell population is maintained to guide new therapies.

The β cell population is believed to be maintained mainly through proliferation (Dor et al., 2004). However, there is evidence of β cell neogenesis from non-β cell sources in the injured adult murine pancreas (Chera et al., 2014; Thorel et al., 2010; Xu et al., 2008), although the existence and significance of endocrine progenitors in homeostasis of the adult pancreas remain disputed.

Expression of Ngn3, a key transcription factor expressed in endocrine progenitors of the developing pancreas (Gradwohl et al., 2000), has been strongly implicated in adult β cell neogen-

esis. Ductal cells have been proposed as a source of adult Ngn3+ cells. Deletion of the E3 ubiquitin ligase Fbw7, which controls the stability of Ngn3, in adult ductal cells (Sancho et al., 2014) and overexpression of the transcription factor Pax4 in α (Al-Hasani et al., 2013) and δ cells (Druelle et al., 2017) has uncovered ductal plasticity, where ductal cells can become endocrine cells via Ngn3 expression. However, lineage tracing strategies have produced conflicting evidence for the ability of ductal cells to generate β cells in homeostasis and in injury paradigms. Use of carbonic anhydrase II (CAII)-CreERT with a R26-LacZ tracer suggests that endocrine cells can be derived from ductal cells following the injury model of pancreatic duct ligation (PDL) (Inada et al., 2008). Use of the Sox9-CreERT with a Rosa26-mT/mG tracer labels 90% of ductal cells, and traced β cells can be observed after hyperglycemia and cytokine treatment (Zhang et al., 2016). In contrast, use of promoters such as Krt19, Mucin1, Sox9, Hes1 and Hnf1b has not shown ductal contribution to β cell regeneration (Kopinke et al., 2011; Kopinke and Murtaugh, 2010; Means et al., 2008; Solar et al., 2009). Likewise, dilution of labeled β cells
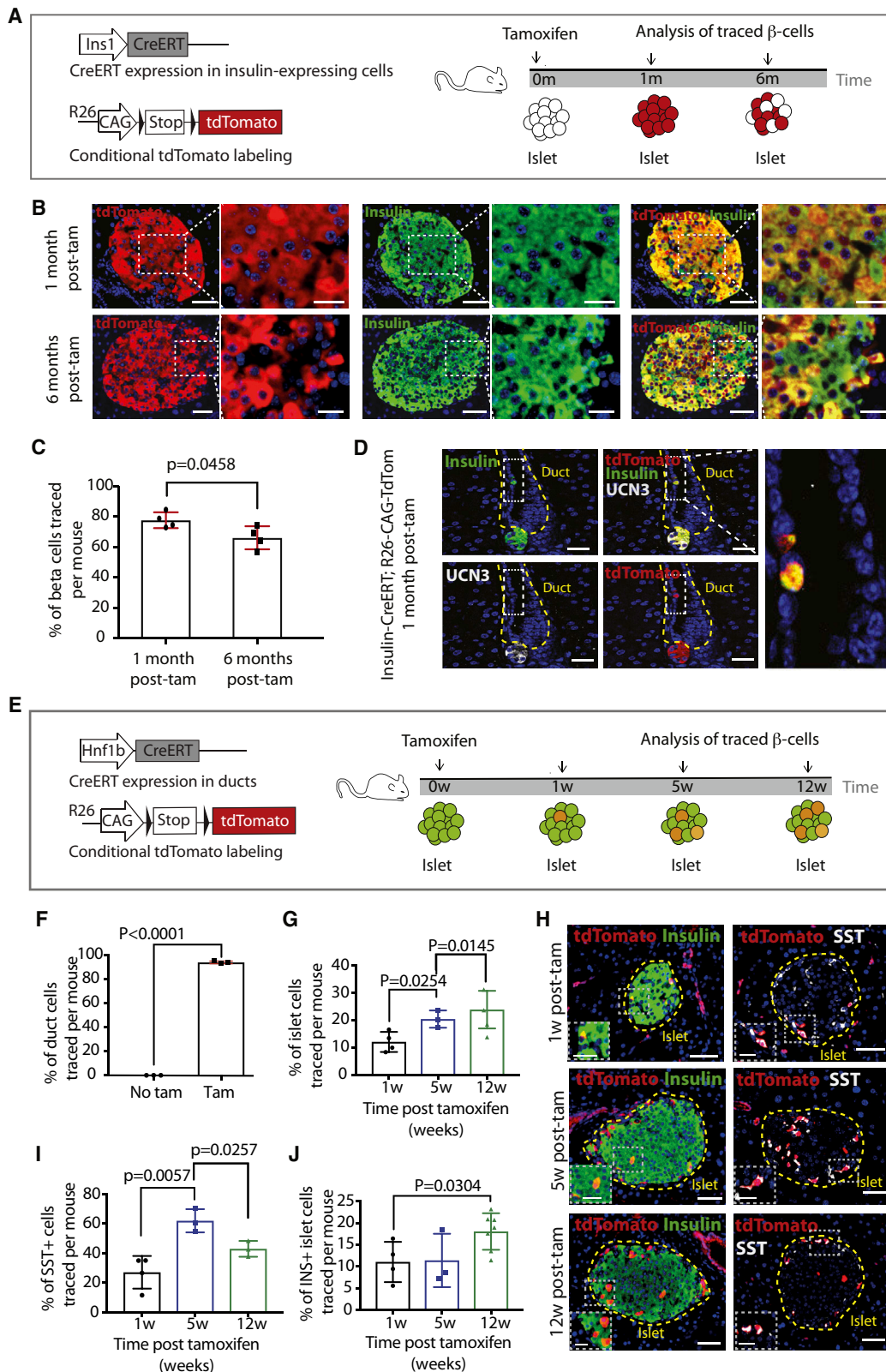
over time in homeostasis and after PDL has been reported (Van de Casteele et al., 2013), but has not been seen in other studies (Dor et al., 2004; Zhao et al., 2021). Thus, the question of whether ductal cells can differentiate into endocrine cells is controversial and unresolved. Differences in expression of promoters used to drive Cre expression in ductal cells and the recombination efficiencies of the tracers used results in great discrepancy of labeling efficiency. Moreover, the duration for which the labeled cells were followed has been highly variable. These technical issues may explain some of the contradictory results observed. Thus, although there is some evidence of adult duct-derived endocrine differentiation, its role and significance are unclear.

Here, by taking advantage of technology improvements in lineage tracing and 3D imaging, we demonstrate that ductal cells contribute to the islet β cell population in homeostasis and during diabetes. Use of the Hnf1b-CreERT driver and R26-CAG-TdTomato lineage tracer enabled efficient, nearly complete labeling of ductal cells. A subpopulation of ductal cells has been found to express Ngn3 (Ngn3+) and also expressed somatostatin (SST+). Additionally, through the use of 3D imaging, Ngn3-traced cells co-expressing insulin (INS) and SST (INS+/SST+) were observed within and between ducts and islets. Single-cell RNA sequencing (scRNA-seq) analysis of Ngn3-traced islets predicted a trajectory where Ngn3+ cells become SST+ cells, which, in turn, become INS+ β cells. Our analyses demonstrate the existence of a rare ductal Ngn3+ population that contributes to the maintenance of islet cell populations.

RESULTS

Non-β cells contribute to the islet β cell population during homeostasis

To follow INS+ cells over time, we crossed the Ins1-CreERT line (Wicksteed et al., 2010) to the sensitive lineage tracer R26-CAG-TdTomato (Madisen et al., 2010; Figure 1A). Adult mice were analyzed 1 and 6 months after tamoxifen (Figure 1A), and the pancreas was analyzed by antibody staining, scanning, and automated quantification to determine the percentage of islet β cells traced (Figures S1A and S1B; Tables S1 and S2). We observed a significant decrease in tracing from 78% to 66% between 1 and 6 months after tamoxifen injection (Figures 1B and

1C), suggesting dilution of existing islet β cells of 0.68% per week. Traced INS+ cells were found outside of the islets (Figure 1D), including within ducts, but they were negative for the mature β cell marker Urocortin3 (UCN3), suggesting that these duct-resident INS+ cells may be immature. This indicates that INS+/UCN3− cells exist outside of the islets and may contribute to the β cell population over time.

Ductal cells contribute to the β cell population over time

Ductal cells are a candidate population that may account for the dilution of the INS+ islet population over time (Sancho et al., 2014; Figure 1C). To circumvent potential issues caused by the low lineage tracing efficiencies seen in earlier studies, we used Hnf1b-CreERT; R26-CAG-TdTomato mice (Figure 1E). 94% of ductal cells were labeled following tamoxifen administration (Figure 1F). Labeling of some δ (SST+) cells was observed (Figures 1H and 1I), as well as labeling of isolated cells found outside of the islets and ducts (Figures S1C and S1D). Islets were analyzed 1, 5, and 12 weeks after tamoxifen (Figures 1G and 1H). We observed a significant increase in the percentage of lineage-traced islet cells between 1 and 5 weeks, which only slightly increased further at the 12-week time point (Figure 1G). More than 90% of traced cells in the islets expressed INS or SST. Traced SST+ cells increased significantly between 1 and 5 weeks and accounted for the majority of tdTomato+ traced cells 5 weeks after tamoxifen, but a sharp decrease was observed 12 weeks after tamoxifen (Figure 1I). The percentage of traced β (INS+) cells was unaltered between 1 week and 5 weeks after tamoxifen but showed a significant increase between 5 and 12 weeks after tamoxifen (Figure 1J), corresponding to the decrease in traced δ cells. Over 12 weeks, this accounted for an increase of 0.66% of traced β cells per week, very similar to the rate of dilution found in the Ins1-CreERT; R26-CAG-tdTomato experiment (Figure 1C). These data suggest that an influx of Hnf1b-traced cells into the islet occurs over time, which contributes to maintaining the β cell population.

Ductal Ngn3+ cells are present in the adult pancreas and express SST

Ductal cells have been shown to be able to transdifferentiate to β cells upon forced expression of transcription factors, including Ngn3 (Al-Hasani et al., 2013; Sancho et al., 2014; Vieira et al.,

Figure 1. The β cell population is not solely maintained by existing β cell proliferation

(A) Lineage tracing strategy and experimental timeline.

(B) Double immunofluorescence (IF) for tdTomato and INS in INS-CreERT; R26-CAG-tdTomato mice 1 and 6 months after tamoxifen, with high magnification shown on the right. Scale bars, 50 μm (left) and 20 μm (right).

(C) Quantification of the percentage of INS+ islet cells traced per mouse (N = 4) at both time points (10–26 weeks of age at injection). Data are represented as mean with SD and p value is indicated.

(D) Triple IF for tdTomato, INS and Urocortin3 (UCN3). A traced ductal INS+/UCN3− (boxed) is shown at high magnification. Scale bars, 25 μm (left) and 10 μm (right).

(E) Lineage tracing strategy and experimental workflow.

(F) Quantification of the percentage of ductal cells labeled 1 week after tamoxifen (N = 3 at 8 weeks of age at injection). Data are represented as mean with SD and p values are indicated.

(G) Quantification of the percentage of islet cells traced per mouse. N = 4 at each time point (8–16 weeks of age at injection). Data are represented as mean with SD and p values are indicated.

(H) Double IF for tdTomato/INS and tdTomato/SST. High magnification is shown in the inset (white dashed line). Scale bars, 50 μm.

(I) Quantification of the percentage of SST+ islet cells traced per mouse. N = 4 at each time point (8–16 weeks of age at injection). Data are represented as mean with SD and p values are indicated.

(J) Quantification of the percentage of INS+ islet cells traced per mouse. N = 4 at each time point (8–16 weeks of age at injection). Data are represented as mean with SD and p values are indicated.
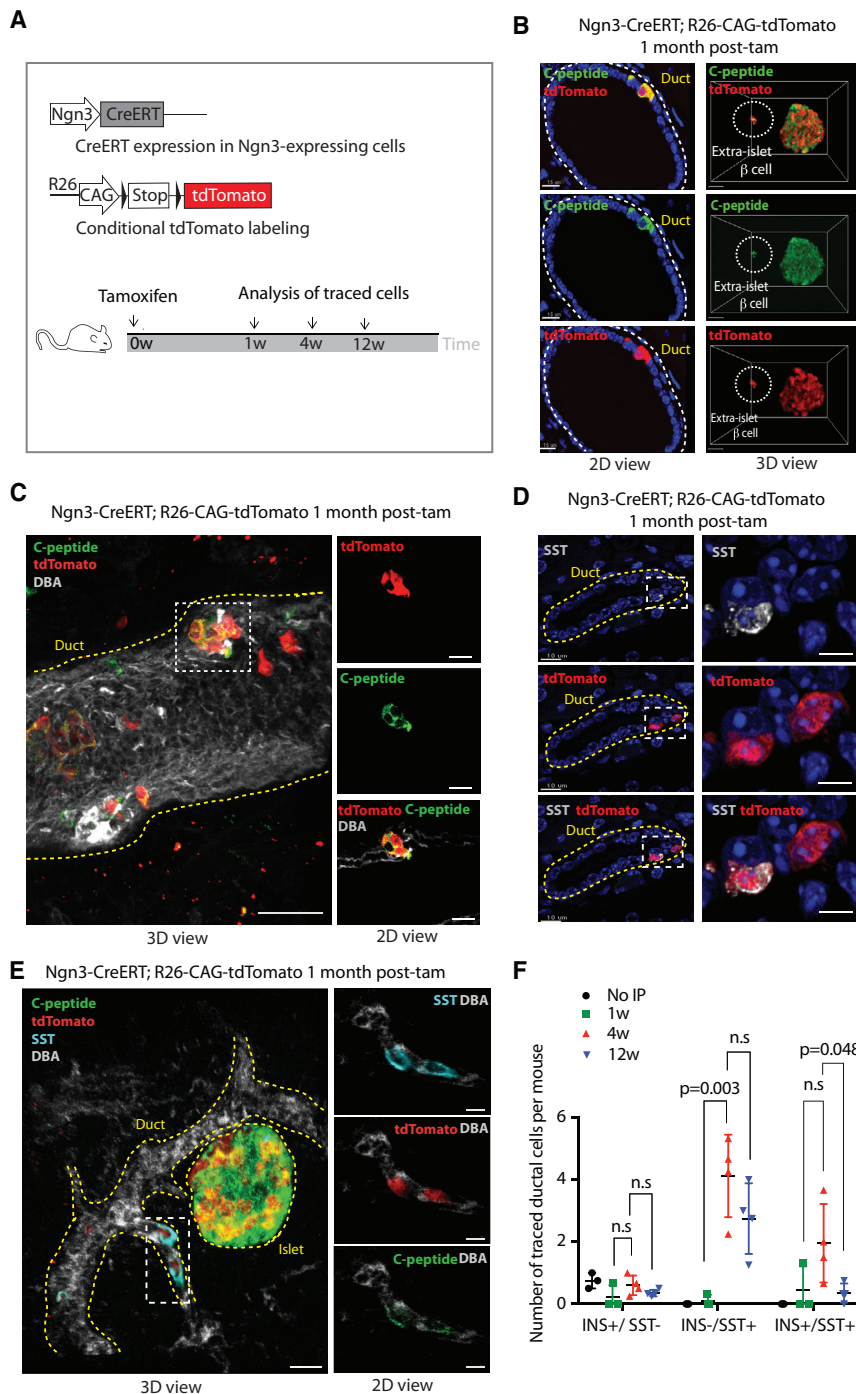
See also Figure S1.

CellPress
OPEN ACCESS

A Ngn3 CreERT

CreERT expression in Ngn3-expressing cells

R26 CAG Stop tdTomato

Conditional tdTomato labeling

Tamoxifen   Analysis of traced cells

0w   1w   4w   12w   Time

B Ngn3-CreERT; R26-CAG-tdTomato
1 month post-tam

C-peptide tdTomato   Duct   C-peptide tdTomato / Extra-islet β cell

C-peptide   Duct   C-peptide / Extra-islet β cell

tdTomato   Duct   tdTomato / Extra-islet β cell

2D view   3D view

C Ngn3-CreERT; R26-CAG-tdTomato 1 month post-tam

C-peptide tdTomato DBA   Duct   tdTomato / C-peptide / tdTomato C-peptide DBA

3D view   2D view

D Ngn3-CreERT; R26-CAG-tdTomato
1 month post-tam

SST   Duct   SST
tdTomato   Duct   tdTomato
SST tdTomato   Duct   SST tdTomato

E Ngn3-CreERT; R26-CAG-tdTomato 1 month post-tam

C-peptide tdTomato SST DBA   Duct   Islet   SST DBA / tdTomato DBA / C-peptide DBA

3D view   2D view

F

Number of traced ductal cells per mouse

● No IP ■ 1w ▲ 4w ▼ 12w

n.s   n.s   p=0.003   n.s   n.s   p=0.048

INS+/ SST-   INS-/SST+   INS+/SST+

Figure 2. Ngn3-labeled cells found in ducts in homeostasis express SST

(A) Lineage tracing and experimental timeline.
(B) Left: double IF for tdTomato and C-peptide in Ngn3-CreERT; R26-CAG-tdTomato mice, showing a C-peptide+/tdTomato+ cell in a duct. Scale bar, 15 μm. Right: 3D view following FLASH for tdTomato and C-peptide, showing an extra-islet C-peptide+/tdTomato+ cell. Scale bar, 20 μm.
(C) 3D view following FLASH for tdTomato, C-peptide, and *Dolichos biflorus* agglutinin (DBA). An islet-like structure associated with the ductal epithelium is boxed. 3D view scale bar, 40 μm; 2D view scale bar, 20 μm.
(D) Double IF for tdTomato and SST, with enlargement shown on the right. Scale bars, 10 μm (left) and 5 μm (right).
(E) 3D view following FLASH for tdTomato, C-peptide, SST, and DBA in an Ngn3-CreERT; R26-CAG-tdTomato mouse pancreas 1 month after tamoxifen. Quadruple-positive cells within the duct (white box) are shown enlarged as a single slice. Scale bars, 40 μm (3D view) and 7 μm (2D views).
(F) Quantification of traced ductal cells per mouse at the listed time points after tamoxifen that are INS+/SST−, INS−/SST+, or INS+/SST+. N = 3 "no intraperitoneal (IP) tamoxifen injection ," N = 3 at 1 week, N = 4 at 4 weeks, and N = 4 at the 12 week time point. The average of 4 sections per mouse is shown. Data are represented as mean with SD and p values are indicated; n.s (p>0.05).
See also Figure S2 and Videos S1 and S2.

S2A). In the ducts, mini-islet-like clusters of cells positive for the β cell marker C-peptide were found (Figures 2C and S2B). Moreover, imaging revealed cells in ducts that expressed the δ cell marker SST (Figure 2D) and often co-expressed C-peptide and INS (Figure 2E; Video S1). Quantification of traced ductal cells revealed that the large majority of duct-resident traced cells were positive for SST and only very rarely INS+/SST− (Figure 2F). More hormone-expressing Ngn3-traced ductal cells were observed 4 weeks after tamoxifen compared with 12 weeks after tamoxifen, suggesting that these cells may leave the ducts over time (Figure 2F). 3D imaging revealed SST+ traced cells that lowly expressed C-peptide located between a duct and islet (Figure S2A; Video S2). The location and elongated morphology of these cells supports the possibility that these cells might be migratory. These data suggest that a small population of ductal cells expresses Ngn3 and endocrine markers, predominantly SST, and that these may have the ability to leave the ductal epithelium.

Ngn3+ ductal cell numbers are increased in diabetes
The putative contribution of ductal Ngn3+ cells to maintaining the β cell population in homeostasis is likely minor compared with

2018), so we reasoned that, if ductal cells were to give rise to β cells, then Ngn3 expression should be necessary. To analyze the differentiation potential and progeny of Ngn3+ cells, we used Ngn3-CreERT; R26-CAG-tdTomato mice (Figure 2A). Ngn3-traced cells were observed in the ducts and islets and often expressed endocrine markers (Figure 2B, left panel). 3D fast light-microscopic analysis of antibody-stained whole organs(FLASH) imaging of the pancreas (Messal et al., 2019) revealed traced cells located outside of ducts and islets (Figures 2B, right panel, and
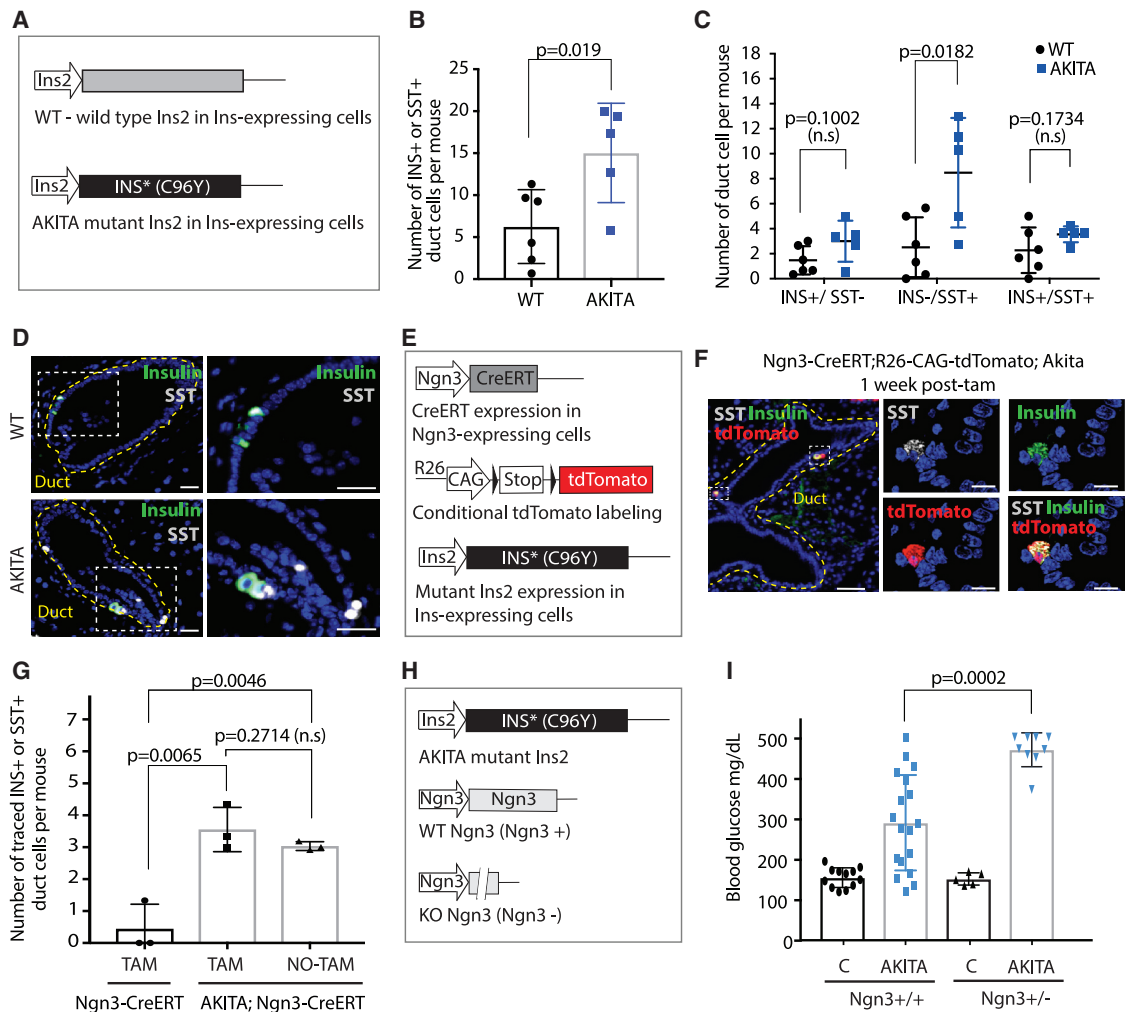
Figure 3. Ngn3+ ductal cell contribution to the endocrine cell population is increased during diabetes

(A) Schematic of the AKITA model of diabetes.

(B) Quantification of SST+ or INS+ duct cells per mouse in age-matched (8–12 weeks of age) control (wild type [WT]) or diabetic (AKITA) mice. N = 6 WT and N = 5 AKITA. Diabetic mice exhibited non-fasting blood glucose of 350–500 mg/dL. Data are represented as mean with SD and p values are indicated.

(C) Quantification of ductal cells per mouse in WT or AKITA (diabetic) mice that are INS+/SST−, INS−/SST+, or INS+/SST+. N = 6 WT and N = 5 AKITA. The average of 4 sections per mouse is shown. Data are represented as mean with SD and p values are indicated

(D) Double IF for INS and SST in WT and AKITA. Hormone-expressing ductal cells are shown enlarged (boxed). Scale bars, 25 μm.

(E) Schematic of strategy to label Ngn3-expressing cells in AKITA mice.

(F) Triple IF for INS, SST, and tdTomato. Hormone-expressing cells near the ductal epithelium are shown enlarged (boxed). Scale bars, 50 μm (left) and 10 μm (right).

(G) Quantification of traced SST+ or INS+ duct cells per mouse in age-matched Ngn3-CreERT tamoxifen-injected (N = 3), AKITA; Ngn3-CreERT tamoxifen-injected (N = 3), and Ngn3CreERT non-injected (N = 4) mice. Mice were injected at 8–12 weeks of age and analyzed 1 week after tamoxifen. Data are represented as mean with SD and p values are indicated.

(H) Schematic of the breeding strategy. $Akita^{+/-}$ mice were crossed to $Ngn3^{+/-}$ mice.

(I) Non-fasted blood glucose levels in mice of listed genotypes measured at 7 weeks of age. Control $Ngn3^{+/+}$, N = 12, AKITA $Ngn3^{+/+}$, N = 18; control $Ngn3^{+/-}$, N = 5; AKITA $Ngn3^{+/-}$, N = 9. Data are represented as mean with SD and p values are indicated.

See also Figure S2.

proliferation because the dilution of traced β cells was small (Figure 1C). To determine whether Ngn3+ cells play a larger role in responding to increased β cell demand, we used the AKITA model of diabetes. AKITA mice harbor a point mutation in the *Ins2* gene (Yoshioka et al., 1997; Figure 3A) that causes misfolding of INS and gradual β cell death (Ron, 2002). SST+ or INS+ ductal cells were more common in diabetic mice compared with controls

(Figure 3B), with more INS−/SST+ ductal cells found in AKITA mice (Figures 3C and 3D). To further investigate the importance of Ngn3+ cells in the diabetic context, Ngn3-CreERT; R26-CAG-TdTomato; AKITA mice were generated (Figure 3E). Following tamoxifen administration, a substantial increase in traced INS+ or SST+ cells found in ducts was observed in diabetic mice (Figures 3F and 3G). This suggested that the number
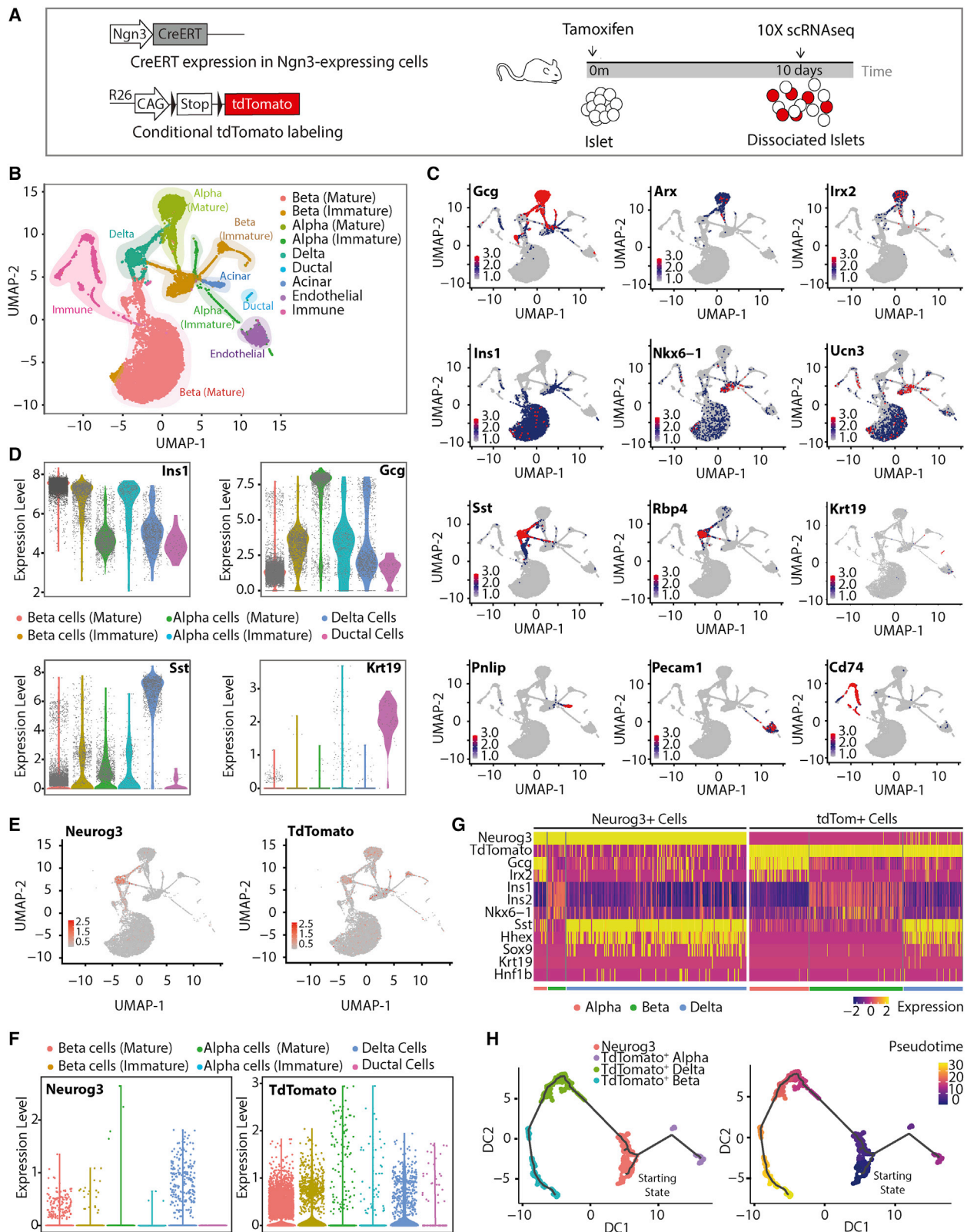
of duct-resident Ngn3+ cells increases during diabetes. To assess the relevance of Ngn3+ cells in diabetes, one allele of *ngn3* was inactivated in an AKITA background (Figure 3H). *ngn3* heterozygosity did not affect blood glucose levels or β cell area in wild-type mice (Figures 3I, S2C, and S2D). As expected, 80% of AKITA males were hyperglycemic at 7 weeks of age, with an average blood glucose level of 292 mg/dL (Figure 3I). Heterozygous loss of *ngn3* in AKITA mice worsened the phenotype, with all animals being diabetic and exhibiting very high average blood glucose values of 473 mg/dL (Figures 3H and 3I). These data suggest that endocrine neogenesis from Ngn3+ ductal cells is enhanced during diabetes, which may be a regenerative response to β cell loss.

β Cell mass is known to increase during pregnancy (Kim et al., 2010). Lineage tracing was initiated in Hnf1b-CreERT; R26-CAG-TdTomato mice, followed by mating to induce pregnancy (Figures S2E and S2F). However, the percentages of lineage-traced INS+ β cells were actually decreased by pregnancy, suggesting that the β cell mass increase in pregnancy is not mediated by ductal endocrine progenitors (Figures S2E–S2H).

Single-cell transcriptomics identifies a Ngn3+/SST+ population able to differentiate to β cells

Because our data suggest that Ngn3+ ductal cells contribute to the islet endocrine cell population over time (Figures 1 and 2), we decided to analyze Ngn3-traced islet cells to determine their origin. To this end, we performed scRNA-seq of islets isolated from Ngn3-CreERT; R26-CAG-tdTomato mice 10 days after tamoxifen (Figure 4A), a time point when traced cells are observed in the islets and neogenesis may have occurred.

Following isolation, islets were dissociated to single cells and processed for transcriptomic analysis using 10X Chromium technology. After quality control steps, our dataset contained 21,813 cells (Figure S3). Following principal-component analysis (PCA), uniform manifold approximation and projection (UMAP) was performed, which revealed distinct clusters (Figure 4B). The identity of these clusters was allocated based on the expression of *bona fide* markers for β (Ins1), α (Gcg), δ (Sst), ductal (Krt19), immune (Cd74), and endothelial cells (Pecam1) (Figures 4B–4D and S3). Further analysis of the expression of markers for each cell type confirmed accurate cluster identities (Figure 4C). Interestingly, the β cell cluster (Ins1+ cells) subdivided into Ucn3^{low}/Ins1^{low} (immature β cells) and Ucn3^{high}/Ins1^{high} (mature β cell) populations, and the α cell cluster contained Gcg^{high} (mature) and Gcg^{low} (immature) cells, suggesting heterogeneity in these endocrine populations (Figures 4D and S3). Ngn3+ cells (n = 227) and tdTomato+ cells (n = 365) were identified within the dataset (Figure 4E). Strikingly, although Ngn3+ cells were mostly found within the δ cell cluster, tdTomato+ cells were mainly clustered in the mature β cell group (Figure 4F). The tdTomato+ β cell transcriptome was indistinguishable from the transcriptome of mature tdTomato– β cells from our dataset and from previous published datasets (Figures S4A and S4B) and they expressed the mature β cell markers C-peptide and UCN3 (Figures S4C and S4D). Expression of Ngn3 in tdTomato cells was minimal 10 days after tamoxifen, indicating that expression of Ngn3 is transient. Further analysis of gene expression associated with the different islet cell types in Ngn3+ or tdTomato+ cells demonstrated that both groups exhibit distinct signatures, with the ductal markers Hnf1b and Sox9 found to be expressed in some Ngn3+ and tdTomato+ cells, suggesting a ductal origin (Figure 4G). To address whether we could infer the lineage path of the traced β cells based on individual single-cell transcriptomic signatures, we performed a pseudotime trajectory analysis (Trapnell et al., 2014) on Ngn3+/tdTomato+ cells. Interestingly, a lineage trajectory was predicted where Ngn3+ cells (starting state) give rise to tdTomato+ α (Gcg+) cells and tdTomato+ δ (Sst+) cells and where the latter are precursors of tdTomato+ β (Ins+) cells (Figure 4H). Thus, this analysis is in agreement with our lineage-tracing studies (Figures 1I–1L), which suggested that duct-derived SST+ δ cells give rise to β cells in the adult pancreas.

DISCUSSION

Here we show that β cell neogenesis occurs in the adult pancreas from Ngn3-traced ductal cells. Immunofluorescence analysis of paraffin sections and analysis of the pancreas by 3D FLASH imaging, complemented by scRNA-seq of islets containing cells traced from Ngn3+ cells, indicates that Ngn3+ cells can become INS+ cells via an intermediate SST+ state. Higher numbers of hormone-positive ductal cells traced from Ngn3+ cells were observed in diabetic mice, and heterozygous loss of Ngn3 accelerated diabetes onset. The adult β cell population is believed to be maintained mainly by proliferation, but our study identified a second physiologically important mechanism of β cell neogenesis.

Our lineage tracing of β cells suggested that some β cells are not derived from β cell replication over time (0.68% of β cells per week) (Figure 1C). Use of Hnf1b-CreERT; R26-CAG-tdTomato mice resulted in labeling of 94% of ductal cells (Figure 1F), and an increased contribution of Hnf1b-expressing cells to the β cell population over time was observed (Figures 1H and 1J). This accounted for 0.66% of β cells per week, strikingly similar to the rate of dilution of β cells traced by Ins1-CreERT (Figure 1C).

Figure 4. scRNA-seq analysis reveals an adult Ngn3+ population able to differentiate into endocrine cells
(A) scRNA-seq experimental design.
(B) UMAP projection of 21,813 pancreatic islet cells. Cells are colored by assigned cluster.
(C) Expression of α (Gcg, Arx, and Irx2), β (Ins1, Nkx6-1, and Ucn3), δ (Sst and Rbp4), ductal (Krt19), acinar (Pnlip), endothelial (Pecam1), and immune (Cd74) cell markers across the scRNA-seq dataset.
(D) Violin plots for expression of Ins1, Gcg, Sst, and Krt19 across identified clusters.
(E) UMAP projection of Ngn3 (Neurog3) and tdTomato expression across a single-cell dataset.
(F) Violin plots for expression of Ngn3 in Ngn3+ cells (left) and tdTomato in tdTomato+ cells (right) across the identified clusters.
(G) Expression heatmap of α, β, δ, and ductal cells markers across Ngn3+ and tdTomato+ cells.
(H) Monocle 3.12 pseudotime analysis of Ngn3+ and tdTomato+ cells (left, predicted lineage trajectories; right, pseudotime projection in the predicted trajectories).
See also Figure S3.

Because δ cell labeling was also observed using the Hnf1b-CreERT lineage tracer (Figure 1I), we cannot rule out a contribution of islet δ cells to the traced β cell population over time. However, the percentage of tdTomato-labeled islet cells increased significantly over time (Figure 1G), suggesting that an influx of traced cells from outside of the islet occurred. The percentage of SST+-labeled cells dropped 12 weeks after tamoxifen injection, which coincided with a significant increase of labeled β cells observed at 12 weeks (Figures 1I and J). This is consistent with differentiation of duct-derived SST+ cells into β cells, corroborated by the lineage trajectory inferred from scRNA-seq (Figure 4H). It has been reported that ectopic expression of Pax4 in pancreatic δ cells results in β-like cell neogenesis (Druelle et al., 2017); our results suggest that this transdifferentiation process also occurs physiologically to maintain the β cell population.

We observed Ngn3-traced bi-hormonal (INS+/SST+) and mono-hormonal (INS+ or SST+) cells within ducts that were sometimes aggregated in small islet-like clusters (Figures 2C and S2B). Furthermore, scRNA-seq suggested a ductal origin of some of the traced islet cells and predicted INS+/SST+ cells as intermediates to the newly formed β cells (Figure 4H). This suggests that the pancreatic ducts harbor a progenitor cell population capable of differentiation into different endocrine cell types.

Contribution of ductal cells to the islet population requires cell migration. 3D imaging revealed traced Ngn3+ cells and INS+/SST+ cells located between ducts and islets (Figure S2A; Video S2), as would be predicted for duct-derived endocrine progenitor cells migrating toward the islets. Thus, our study suggests that β cell neogenesis can occur from the ductal compartment in homeostasis (Figure S4E).

The acceleration of diabetic onset in $Akita^{+/-} Ngn3^{+/-}$ mice, combined with increased numbers of Ngn3-traced INS+/SST+ ductal cells in diabetic mice (Figure 3), suggests that Ngn3-mediated adult β cell neogenesis is enhanced in diabetes. Ductal cells have been considered a potential source of β cells in humans because of observations of endocrine cells within the ductal epithelium, with INS+ ductal cells observed, especially in obese individuals (Butler et al., 2003). Further characterization of adult endocrine neogenesis may reveal mechanisms and enable harnessing of this physiological β cell source, which could be employed for the benefit of individuals with diabetes.

Limitations of study

In this study, we identified Ngn3+ ductal progenitors as a source of adult β cell neogenesis. We only analyzed these cells up to 8 months in age in mice, and it is conceivable that the contribution of duct-derived β cell neogenesis changes with age. Longer-term lineage tracing is needed to address this.

Although the concept of exploiting this progenitor population for diabetes treatment is attractive, these SST+ ductal endocrine progenitors remain uncharacterized. Approaches like scRNA-seq of the ductal compartment, focusing on SST+ ductal cells, is necessary to further characterize these cells before our findings can be exploited therapeutically.

STAR★METHODS

Detailed methods are provided in the online version of this paper and include the following:

- KEY RESOURCES TABLE
- RESOURCE AVAILABILITY
  - Lead contact
  - Materials availability
  - Data and code availability
- EXPERIMENTAL MODEL AND SUBJECT DETAILS
  - Animal models
- METHOD DETAILS
  - Processing tissue for immunofluorescent (IF) staining
  - Immunofluorescent (IF) staining of sections
  - FLASH (3D-IF staining)
  - Imaging
  - Preparing islet cells for single cell RNA-sequencing
  - scRNAseq Library Preparation and Sequencing
  - Generation of single cell expression matrix
  - scRNAseq Quality Control and Cell Filtering
  - Dimensionality Reduction, UMAP Visualization and Clustering Analysis
  - Differential Expression Analysis and Cluster Identification
  - Pseudotime Trajectory Analysis
- QUANTIFICATION AND STATISTICAL ANALYSIS
  - Percentage of islet beta cells traced
  - Ductal labeling efficiency
  - INS+ and SST+ cells in ducts

AUTHOR CONTRIBUTIONS

C.G., C.L., R.S., and A.B. conceived the study, analyzed data, and wrote the paper. C.G. performed lineage tracing, C.G. and C.L. performed immunofluorescence, C.L. performed the single-cell analysis, I.E. assisted with the *in vivo* experiments, H.A.M. developed and performed the FLASH imaging, C.R. and E.-L.H. performed islet isolation for RNA-seq, and H.H. and P.J. assisted with study design and interpretation.

DECLARATION OF INTERESTS

The authors declare no competing interests.

REFERENCES

Al-Hasani, K., Pfeifer, A., Courtney, M., Ben-Othman, N., Gjernes, E., Vieira, A., Druelle, N., Avolio, F., Ravassard, P., Leuckx, G., et al. (2013). Adult duct-lining cells can reprogram into β-like cells able to counter repeated cycles of toxin-induced diabetes. Dev. Cell *26*, 86–100.

Amezquita, R.A., Lun, A.T.L., Becht, E., et al. (2020). Orchestrating single-cell analysis with Bioconductor. Nat. Methods *17*, 137–145. https://doi.org/10.1038/s41592-019-0654-x.

Andrews, S. (2010). FastQC: a quality control tool for high throughput sequence data (Babraham Bioinformatics).

Butler, A.E., Janson, J., Bonner-Weir, S., Ritzel, R., Rizza, R.A., and Butler, P.C. (2003). Beta-cell deficit and increased beta-cell apoptosis in humans with type 2 diabetes. Diabetes *52*, 102–110.

Chera, S., Baronnier, D., Ghila, L., Cigliola, V., Jensen, J.N., Gu, G., Furuyama, K., Thorel, F., Gribble, F.M., Reimann, F., and Herrera, P.L. (2014). Diabetes recovery by age-dependent conversion of pancreatic δ-cells into insulin producers. Nature *514*, 503–507.

Dobin, A., Davis, C.A., Schlesinger, F., Drenkow, J., Zaleski, C., Jha, S., Batut, P., Chaisson, M., and Gingeras, T.R. (2013). STAR: ultrafast universal RNA-seq aligner. Bioinformatics *29*, 15–21.

Dor, Y., Brown, J., Martinez, O.I., and Melton, D.A. (2004). Adult pancreatic beta-cells are formed by self-duplication rather than stem-cell differentiation. Nature *429*, 41–46.

Druelle, N., Vieira, A., Shabro, A., Courtney, M., Mondin, M., Rekima, S., Napolitano, T., Silvano, S., Navarro-Sanz, S., Hadzic, B., et al. (2017). Ectopic expression of *Pax4* in pancreatic δ cells results in β-like cell neogenesis. J. Cell Biol. *216*, 4299–4311.

Gradwohl, G., Dierich, A., LeMeur, M., and Guillemot, F. (2000). neurogenin3 is required for the development of the four endocrine cell lineages of the pancreas. Proc. Natl. Acad. Sci. USA *97*, 1607–1611.

Gu, G., Dubauskaite, J., and Melton, D.A. (2002). Direct evidence for the pancreatic lineage: NGN3+ cells are islet progenitors and are distinct from duct progenitors. Development *129*, 2447–2457.

Inada, A., Nienaber, C., Katsuta, H., Fujitani, Y., Levine, J., Morita, R., Sharma, A., and Bonner-Weir, S. (2008). Carbonic anhydrase II-positive pancreatic cells are progenitors for both endocrine and exocrine pancreas after birth. Proc. Natl. Acad. Sci. USA *105*, 19915–19919.

Ji, Z., and Ji, H. (2016). TSCAN: Pseudo-time reconstruction and evaluation in single-cell RNA-seq analysis. Nucleic Acids Res. *44*, e117.

Kharroubi, A.T., and Darwish, H.M. (2015). Diabetes mellitus: The epidemic of the century. World J. Diabetes *6*, 850–867.

Kim, H., Toyofuku, Y., Lynn, F.C., Chak, E., Uchida, T., Mizukami, H., Fujitani, Y., Kawamori, R., Miyatsuka, T., Kosaka, Y., et al. (2010). Serotonin regulates pancreatic beta cell mass during pregnancy. 2010. Nat. Med. *16*, 804–808.

Kopinke, D., and Murtaugh, L.C. (2010). Exocrine-to-endocrine differentiation is detectable only prior to birth in the uninjured mouse pancreas. BMC Dev. Biol. *10*, 38.

Kopinke, D., Brailsford, M., Shea, J.E., Leavitt, R., Scaife, C.L., and Murtaugh, L.C. (2011). Lineage tracing reveals the dynamic contribution of Hes1+ cells to the developing and adult pancreas. Development *138*, 431–441.

Lee, C.S., Perreault, N., Brestelli, J.E., and Kaestner, K.H. (2002). Neurogenin 3 is essential for the proper specification of gastric enteroendocrine cells and the maintenance of gastric epithelial cell identity. Genes Dev. *16*, 1488–1497.

Madisen, L., Zwingman, T.A., Sunkin, S.M., Oh, S.W., Zariwala, H.A., Gu, H., Ng, L.L., Palmiter, R.D., Hawrylycz, M.J., Jones, A.R., et al. (2010). A robust and high-throughput Cre reporting and characterization system for the whole mouse brain. Nat. Neurosci. *13*, 133–140.

Martin, M. (2011). Cutadapt Removes Adapter Sequences from High-Throughput Sequencing Reads. EMBnet. J. *17*, 10–12.

McCarthy, D.J., Campbell, K.R., Lun, A.T., and Wills, Q.F. (2017). Scater: pre-processing, quality control, normalization and visualization of single-cell RNA-seq data in R. Bioinformatics *33*, 1179–1186.

McDavid, A., Finak, G., Chattopadyay, P.K., Dominguez, M., Lamoreaux, L., Ma, S.S., Roederer, M., and Gottardo, R. (2013). Data exploration, quality control and testing in single-cell qPCR-based gene expression experiments. Bioinformatics *29*, 461–467.

Means, A.L., Xu, Y., Zhao, A., Ray, K.C., and Gu, G. (2008). A CK19(CreERT) knockin mouse line allows for conditional DNA recombination in epithelial cells in multiple endodermal organs. Genesis *46*, 318–323.

Messal, H.A., Alt, S., Ferreira, R.M.M., Gribben, C., Wang, V.M., Cotoi, C.G., Salbreux, G., and Behrens, A. (2019). Tissue curvature and apicobasal mechanical tension imbalance instruct cancer morphogenesis. Nature *566*, 126–130.

Muraro, M.J., Dharmadhikari, G., Grün, D., Groen, N., Dielen, T., Jansen, E., van Gurp, L., Engelse, M.A., Carlotti, F., de Koning, E.J.P., and van Oudenaarden, A. (2016). A Single-Cell Transcriptome Atlas of the Human Pancreas. Cell Syst. *3*, 385–394.e3.

Ron, D. (2002). Proteotoxicity in the endoplasmic reticulum: lessons from the Akita diabetic mouse. J. Clin. Invest. *109*, 443–445.

Sancho, R., Gruber, R., Gu, G., and Behrens, A. (2014). Loss of Fbw7 reprograms adult pancreatic ductal cells into α, δ, and β cells. Cell Stem Cell *15*, 139–153.

Satija, R., Farrell, J.A., Gennert, D., Schier, A.F., and Regev, A. (2015). Spatial reconstruction of single-cell gene expression data. Nat. Biotechnol. *33*, 495–502.

Solar, M., Cardalda, C., Houbracken, I., Martín, M., Maestro, M.A., De Medts, N., Xu, X., Grau, V., Heimberg, H., Bouwens, L., and Ferrer, J. (2009). Pancreatic exocrine duct cells give rise to insulin-producing beta cells during embryogenesis but not after birth. Dev. Cell *17*, 849–860.

Thorel, F., Népote, V., Avril, I., Kohno, K., Desgraz, R., Chera, S., and Herrera, P.L. (2010). Conversion of adult pancreatic alpha-cells to beta-cells after extreme beta-cell loss. Nature *464*, 1149–1154.

Trapnell, C., Cacchiarelli, D., Grimsby, J., Pokharel, P., Li, S., Morse, M., Lennon, N.J., Livak, K.J., Mikkelsen, T.S., and Rinn, J.L. (2014). The dynamics and regulators of cell fate decisions are revealed by pseudotemporal ordering of single cells. Nat. Biotechnol. *32*, 381–386.

Van de Casteele, M., Leuckx, G., Baeyens, L., Cai, Y., Yuchi, Y., Coppens, V., De Groef, S., Eriksson, M., Svensson, C., Ahlgren, U., et al. (2013). Neurogenin 3+ cells contribute to β-cell neogenesis and proliferation in injured adult mouse pancreas. Cell Death Dis. *4*, e523.

van der Maaten, L., and Hinton, G. (2008). Visualizing data using t-SNE. Machine Learning Research. Machine Learning Research *9*, 2579–2605.

Vieira, A., Vergoni, B., Courtney, M., Druelle, N., Gjernes, E., Hadzic, B., Avolio, F., Napolitano, T., Navarro Sanz, S., Mansouri, A., and Collombat, P. (2018). Neurog3 misexpression unravels mouse pancreatic ductal cell plasticity. PLoS ONE *13*, e0201536.

Wicksteed, B., Brissova, M., Yan, W., Opland, D.M., Plank, J.L., Reinert, R.B., Dickson, L.M., Tamarina, N.A., Philipson, L.H., Shostak, A., et al. (2010). Conditional gene targeting in mouse pancreatic ß-Cells: analysis of ectopic Cre transgene expression in the brain. Diabetes *59*, 3090–3098.

Xu, X., D'Hoker, J., Stangé, G., Bonné, S., De Leu, N., Xiao, X., Van de Casteele, M., Mellitzer, G., Ling, Z., Pipeleers, D., et al. (2008). Beta cells can be generated from endogenous progenitors in injured adult mouse pancreas. Cell *132*, 197–207.

Yoshioka, M., Kayo, T., Ikeda, T., and Koizumi, A. (1997). A novel locus, Mody4, distal to D7Mit189 on chromosome 7 determines early-onset NIDDM in nonobese C57BL/6 (Akita) mutant mice. Diabetes *46*, 887–894.

Zhang, M., Lin, Q., Qi, T., Wang, T., Chen, C.C., Riggs, A.D., and Zeng, D. (2016). Growth factors and medium hyperglycemia induce Sox9+ ductal cell differentiation into β cells in mice with reversal of diabetes. Proc. Natl. Acad. Sci. USA *113*, 650–655.

Zhao, H., Huang, X., Liu, Z., Pu, W., Lv, Z., He, L., Li, Y., Zhou, Q., Lui, K.O., and Zhou, B. (2021). Pre-existing beta cells but not progenitors contribute to new beta cells in the adult pancreas. Nat. Metab. *3*, 352–365.

STAR★METHODS

KEY RESOURCES TABLE

REAGENT or RESOURCE	SOURCE	IDENTIFIER
Antibodies		
Rabbit anti-C-peptide	Cell Signaling	4593 (RRID: AB_10691857)
Goat anti-GFP	Abcam	ab6673 (RRID: AB_305643)
Mouse anti-Insulin	Sigma-Aldrich	I2018 (RRID: AB_260137)
Rabbit anti-RFP	TebuBio	600-401-379 (RRID: AB_2209751)
Rat-anti-Somatostatin	Abcam	ab30788 (RRID: AB_778010)
Goat anti-TdTomato	Biorbyt	Orb182397 (RRID: AB_2687917)
Mouse anti-Urocortin3	Phoenix Pharmaceuticals	Cat# H-019-29
Alexa Fluor 488 donkey anti-mouse	Thermo	A-21202 (RRID: AB_141607)
Alexa Fluor 546 donkey anti-rabbit	Thermo	A10040 (RRID: AB_2534016)
Alexa Fluor 647 goat anti-rat	Thermo	A-21247 (RRID: AB_141778)
Alexa Fluor 488 goat anti-goat	Thermo	A-11055 (RRID: AB_2534102)
Chemicals, peptides, and recombinant proteins		
Fluorescein labeled Dolichos Biflorus Agglutinin (DBA)	Vector labs	FL-1031
Tamoxifen	Sigma	T5648
Peanut oil	Sigma	P2144
Formalin solution, neutral buffered, 10%	Sigma	HT501128
Bovine Serum Albumin	Sigma	A7906
Trisodium citrate dihydrate	Sigma	S1804
Methyl salicylate	Sigma	M6752
Triton X-100	Sigma	T9284
Sudan Black B	Sigma	199664
Methanol	Sigma	32213
Histo-Clear	Fisher	12358637
Deposited data		
scRNA-seq of islet cells from Ngn3-CreERT; R26-CAG-tdTomato mice	This paper	GEO: GSE138038
Experimental models: Organisms/strains		
Mouse: Hnf1bTg(Hnf1b-cre/ERT2)1Jfer	Solar et al., 2009	(RRID: IMSR_JAX:027681)
Mouse: (Tg)(Ins1-cre/ERT)1Lphi	The Jackson Laboratory	Jax: 024709 (RRID: IMSR_JAX:024709)
Mouse: Tg(Neurog3-cre/Esr1*)1Dam	The Jackson Laboratory	Jax: 008119 (RRID: IMSR_JAX:008119)
Mouse: C57BL/6-Ins2Akita/J	The Jackson Laboratory	Jax: 003548 (RRID: IMSR_JAX:003548)
Mouse: tm9.1(CAG-tdTomato)Hze	The Jackson Laboratory	Jax: 007909 (RRID: IMSR_JAX:007909)
Mouse: Neurog3tm1(EGFP)Khk	MMRRC	000344-UCD (RRID: MMRRC_000344-UCD)
Software and algorithms		
StrataQuest Analysis Software	Tissue Gnostics	https://tissuegnostics.com/en/products/analysing-software/strataquest
Zen 2.3	Zeiss	https://www.zeiss.com/microscopy/int/products/microscope-software/zen-lite.html
Imaris 8.3.1	Bitplane	https://imaris.oxinst.com/packages
Cell Ranger 3.2.0	10X Genomics	https://support.10xgenomics.com/single-cell-gene-expression/software/pipelines/latest/installation

(Continued on next page)

REAGENT or RESOURCE	SOURCE	IDENTIFIER
RStudio 3.6.1	RStudio	https://www.rstudio.com/
Prism 7 for MacOS	Graphpad	https://www.graphpad.com/scientific-software/prism/
FastQC	Andrews, 2010	https://www.bioinformatics.babraham.ac.uk/projects/fastqc
Cutadapt	Martin, 2011	https://github.com/marcelm/cutadapt
Scater	McCarthy et al., 2017	https://bioconductor.org/packages/release/bioc/html/scater.html
Seurat	Satija et al., 2015	https://satijalab.org/seurat/
TSCAN	Ji and Ji, 2016(Ji and Ji, 2016)	https://bioconductor.org/packages/release/bioc/html/TSCAN.html
SCE (Single Cell Experiment)	Amezquita et al., 2020(Amezquita et al., 2020)	https://bioconductor.org/packages/release/bioc/html/SingleCellExperiment.html

RESOURCE AVAILABILITY

Lead contact
Further information and requests for resources and reagents should be directed to and will be fulfilled by the lead contact, Axel Behrens (axel.behrens@icr.ac.uk).

Materials availability
This study did not generate new unique reagents.

Data and code availability
All high-throughput sequencing data, both raw and processed files, have been deposited in NCBI's Gene Expression Omnibus and are accessible under accession number GEO: GSE138038.

EXPERIMENTAL MODEL AND SUBJECT DETAILS

Animal models
All animal experiments were approved by the Francis Crick Institute's Animal Welfare and Ethical Review Body and conformed to UK Home Office regulations under the Animals (Scientific Procedures) Act 1986 including Amendment Regulations 2012. Mouse lines used were described previously: Hnf1b-CreERT (MGI: 4420452 Tg(Hnf1b-cre/ERT2)1Jfer) (Solar et al., 2009), Ngn3-CreERT (MGI: 3796205 Neurog3tm1(Neurog3,cre/ERT)Ggu) (Gu et al., 2002), Ins1-CreERT (MGI: 4410453 Tg(Ins1-cre/ERT)1Lphi (Wicksteed et al., 2010), Ngn3$^{+/-}$ (MGI: 2651394 Neurog3$^{tm1(EGFP)Khk}$) (Lee et al., 2002), AKITA (MGI: 1857572 Ins2Akita) (Yoshioka et al., 1997) and Rosa26-CAG-tdTdtomato (MGI: 3809523 Gt(ROSA)26Sortm9(CAG-tdTomato)Hze) (Madisen et al., 2010). For lineage tracing, adult mice (over 8 weeks of age, male and female) were injected intraperitoneally (I.P) with 20 mg/ml tamoxifen at a volume of 5 μL per gram of body weight once daily for 2 days. For blood glucose sampling, a small incision was made at the saphenous vein. Only 1 drop of blood was required. Measurements were recorded using a FreeStyle glucose meter (Abbott), using a FreeStyle disposable strip (Abbott). Non-fasting glucose measurements were performed. Glucose levels were measured at 7 weeks of age in AKITA $^{+/-}$ males and WT male litter mates were used as controls. Details of age and sex of the mice used can be found in Table S1.

METHOD DETAILS

Processing tissue for immunofluorescent (IF) staining
The pancreas was dissected and fixed in 10% NBF (Neutral buffered formalin) overnight. Samples were transferred to 70% ethanol, dehydrated and embedding in paraffin. 4 μm tissue sections were cut using a microtome (RM2235 Leica) and placed in a water bath at 37°C. Sections were then mounted on Superfrost Ultra Plus charged slides and incubated in an oven at 37°C for 15 minutes to encourage adherence.

Immunofluorescent (IF) staining of sections
Slides were dewaxed in HistoClear twice for 5 minutes before being washed in 100% ethanol for 5 minutes. Slides were then passed through a re-hydration series for 5 minutes in each of 95%, 90%, 80% and 50% ethanol, then dH$_2$O. Heat-mediated antigen retrieval was performed using 10mM citrate buffer pH 6.2. The buffer was pre-warmed in a microwave until gently bubbling, before slides were

submerged and heated for 15 minutes in the microwave on 50% power to maintain the temperature of the buffer. Slides were then cooled and washed twice briefly in PBS. Blocking solution containing 1% (w/v) BSA, 5% (v/v) donkey serum and 0.1% (v/v) Triton X-100 was applied to the sections for at least 30 minutes at room temperature in a humidified chamber. Primary antibodies were then diluted in blocking solution and incubated overnight at 4°C in a humidified chamber. Slides were washed for 5 minutes in PBS three times before fluorophore-conjugated secondary antibodies plus DAPI were applied for 45 minutes at room temperature in the humidified chamber. Following this, slides were washed for 5 minutes in PBS three times before being submerged in 0.1% (w/v) Sudan Black B in 70% ethanol (filtered) for 15 minutes at room temperature to reduce autofluorescence. Slides were washed for 5 minutes in PBS three times and mounted in 1 drop of DAKO fluorescent mounting media.

FLASH (3D-IF staining)
FLASH (fast light-microscopic analysis of antibody-stained whole organs) was performed as described (Messal et al., 2019). Cardiac perfusion was performed with 20ml of PBS before tissue was dissected and fixed overnight in 10% NBF at room temperature. The sample was washed in PBT (0.4% Triton X-100 in PBS) 3 times for 1 hour per wash and incubated in antigen retrieval buffer (200mM boric acid plus 4% SDS pH7.0) overnight at 54°C. The sample was washed in PBT 3 times for 1 hour per wash, before being moved to blocking buffer (1% BSA, 5% DMSO, 10% FCS, 0.02% sodium azide and 0.2% Triton X-100) in PBS and incubated overnight at room temperature. Primary antibodies were then incubated in blocking buffer for at least 2 nights at room temperature on a nutator. Samples were washed in PBT 3 times for 1 hour per wash before fluorophore-conjugated secondary antibodies were applied for 2 nights at room temperature on a nutator. Samples were washed in PBS 3 times for 30 minutes per wash and passed through a dehydration series of 30%, 50%, 75% and then 2x 100% methanol for 1h in each solution, protected from light. Dehydrated samples were then gradually cleared by submerging in methyl salicylate diluted in methanol at 25%, 50%, 75% and 2x 100% methyl salicylate for 30 minutes each in a glass dish protected from light. Cleared samples were then mounted on a glass slide in 100% methyl salicylate.

Imaging
For pancreas sections, entire tissue sections were imaged using a Zeiss Axio Scan Z1 slide scanner. A 20x objective was used, detecting signal from Alexa Fluor 488, Alexa Fluor 546 and Alexa Fluor 647-conjugated secondary antibodies, along with DAPI. Multiple images were stitched to form 1 large image file of the complete section that can be navigated using Zen software. Regions of interest were often further imaged manually using a Zeiss upright 710 confocal microscope and a 63x objective. For imaging following FLASH, a Zeiss LSM 780 confocal microscope with a 10x and 25x objective was used. Three-dimensional image analysis was performed using Imaris software. In FLASH images ducts were identified as DBA positive structures. In tissue sections ducts were identified by Hnf1b-tracing and by DAPI staining, which enables identification by ductal morphology. For display purposes images were cropped to display relevant areas.

Preparing islet cells for single cell RNA-sequencing
For the single cell RNA-seq, islets were pooled from six Ngn3-CreERT; R26-CAG-TdTomato mice at 12 weeks of age, at 10 days post-tamoxifen injection. Data was pooled from 2 separate experiments (batch 1 and 2), which included 6 mice in total. Mice were culled by cervical dislocation and the pancreas was perfused with 1mg/ml Collagenase type XI in MEM media. The inflated pancreas was then collected and digested in 1mg/ml Collagenase type XI at 37°C for 10 minutes. Digestion was terminated by adding ice cold complete MEM (MEM plus 10% FCS and 1% P/S) and the sample was centrifuged at 1,400 rpm for 90 s. The pellet was resuspended in complete MEM and spun again to wash the sample. This was repeated 3 times. The suspension was then sieved, centrifuged and resuspended in 15ml of histopaque-1077. 10ml of complete MEM was gently added and the sample was centrifuged at 3,500 rpm for 24 minutes at 4°C with no break. Islets were collected at the histopaque/media interface and washed 3 times in 50ml of complete MEM. Approximately 300 islets were then manually picked using a dissection microscope to increase purity. Islets were pelleted by spinning at 1000 rpm for 5 minutes, resuspended in 1ml of TrypLE express and incubated at 37°C for 20 minutes with occasional pipetting to mix. Reaction was stopped with ice cold PBS and the sample was pelleted. Cells were resuspended in 0.04% BSA and filtered through a 35 μm nylon mesh and processed immediately for single cell RNA-sequencing.

scRNaseq Library Preparation and Sequencing
Cell viability and number were assessed by Trypan blue staining and the Eve automatic cell counter respectively. Approximately 10,000-15,000 cells were loaded into a channel of the 10x Chromium Chip B - according to the 10x Genomics Single Cell 3′ Reagent Kit v3 GEM protocol. RNA was reverse transcribed via 11 PCR cycles, followed by a further 12 PCR cycles for cDNA amplification. Library size was quantified via Agilent TapeStation. scRNaseq library sequencing was performed on the HiSeq 4000 (Illumina) platform, using sequencing parameters: 8-98-28.

Generation of single cell expression matrix
The 10X Genomics Single Cell Software Suite, Cell Ranger 5.0.0 was used to process the scRNaseq data (https://support.10xgenomics.com/single-cell-gene-expression/software/overview/welcome). Demultiplexing was performed based on the 8 bp sample index read to generate FASTQ files for the Read1 and Read2 paired-end reads. Raw reads were pre-processed with the quality control tools FastQC (Andrews, 2010) and Cutadapt (Martin, 2011). Cell Ranger Count aligned reads to the mm10 reference genome via STAR (Dobin et al., 2013). To enable mapping of tdTomato-derived transcripts, the sequence for tdTomato was added

to the reference genome and GTF file. Aligned sequence reads with valid cell barcodes mapping to exons (Ensembl GTF GRCm38.93) were used to generate the gene expression matrix.

scRNaseq Quality Control and Cell Filtering

Using the Bioconductor package Scater 3.9 (McCarthy et al., 2017) low quality cells were removed based upon library size and the number of expressed gene transcripts (Figure S3A). We also removed cells with high mitochondrial read proportion (Figure S3B), indicative of apoptosis. Finally, total cell features were plotted against $\log_{10}$ transformed number of total reads and visible outliers removed (Figure S3C). The scRNaseq dataset (post QC 21813 cells) was a combination of post-QC cells from batch 1 (post QC 1183 cells) and batch 2 (post QC 20630 cells).

Dimensionality Reduction, UMAP Visualization and Clustering Analysis

Cells which passed QC metrics were passed to Seurat 4.0.0 (Satija et al., 2015) for downstream analysis. Normalization was performed using 'regularized negative binomial regression' and the data scaled based upon the top 5000 variable genes. Dimensionality reduction was performed via principal-component analysis (PCA) to enable cell clustering. The top 15 principal components (PCs) were selected – indicated via the inbuilt permutation-based test and passed to Uniform Manifold Approximation and Projection (UMAP) for clustering visualization (van der Maaten and Hinton, 2008). The clustering analysis was performed with a resolution value of 0.5 and cluster number validated by scree plot (Figure S3D).

Differential Expression Analysis and Cluster Identification

Differentially expressed genes between clusters were identified by comparing average intra-cluster expression values against expression in cells of all other clusters using the Seurat DeSeq2 workflow (McDavid et al., 2013) with standard parameters used. The top 10 differentially expressed genes per cluster were used for identification and compared to known marker genes (Muraro et al., 2016) for validation.

Pseudotime Trajectory Analysis

Pseudotime trajectory analysis of Ngn3+ and tdTomato+ cells was performed using the Bioconductor package Monocle 3.12 (Ji and Ji, 2016). In brief, raw counts for Ngn3+ and tdTomato+ cells were subsetted and pre-processed prior to dimensionality reduction via PCA. Cells were clustered to form a minimal spanning tree enabling cell ordering along their predicted trajectory as previously described.

QUANTIFICATION AND STATISTICAL ANALYSIS

All statistics were calculated using GraphPad Prism 7, where unpaired t tests were performed to compare time points. *P value*s are specified in figures.

Percentage of islet beta cells traced

The percentage of INS+ islet cells traced was determined by using a custom-made analysis profile using Strataquest software. Analysis was performed on scanned sections. The software defined multicellular INS+ structures as islets, TdTomato+ cells as traced cells and used DAPI to define single cells. By performing an overlay, the percentage INS+/tdTomato+ islet cells was determined. Data from 4 sections per mouse were averaged and presented per mouse.

Ductal labeling efficiency

To determine the ductal recombination efficiency in Hnf1b-CreERT; R26-CAG-tdTomato mice, manual quantification was performed. Whole pancreas sections were analyzed following IF staining for tdTomato. Ducts were identified based on DAPI staining and morphology. For each duct, each cell was counted and the percentage of cells within a duct that were tdTomato positive was calculated.

INS+ and SST+ cells in ducts

To quantify the number of INS+ and SST+ cells in ducts, whole pancreas sections were scanned following IF for TdTomato, Insulin and SST. The number of ductal cells expressing the markers were then manually counted.

Supplemental Information

Ductal Ngn3-expressing progenitors contribute

to adult β cell neogenesis in the pancreas

Christopher Gribben, Christopher Lambert, Hendrik A. Messal, Ella-Louise Hubber, Chloe Rackham, Ian Evans, Harry Heimberg, Peter Jones, Rocio Sancho, and Axel Behrens
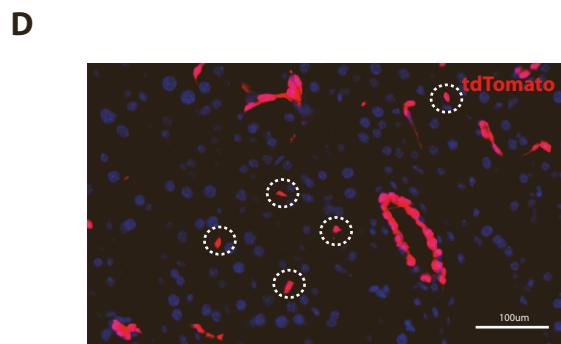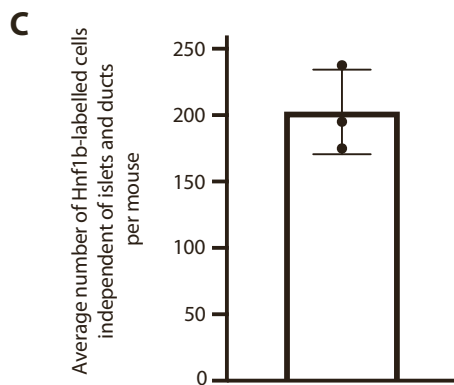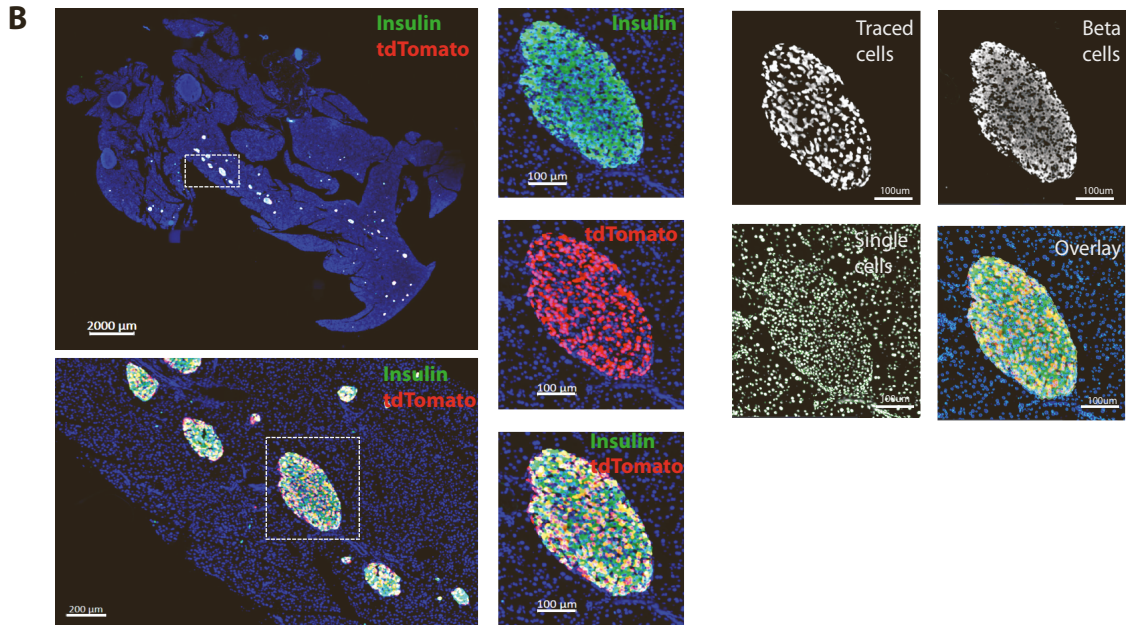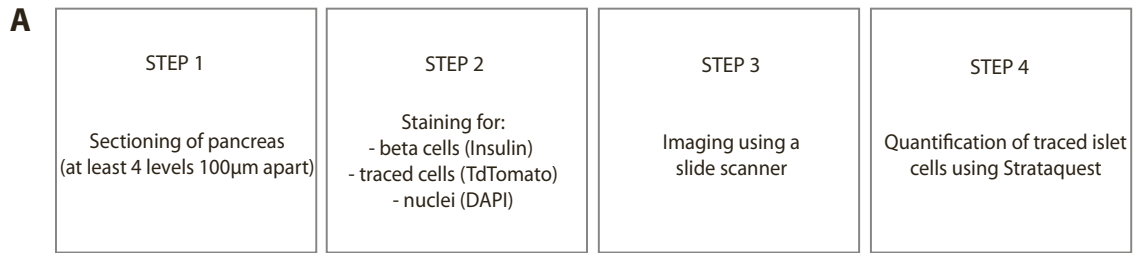
Figure S1: Scheme of lineage tracing analysis and quantification, related to Figure 1

A) Workflow of processing, antibody staining, fluorescent imaging and analysis.
B) Double IF for Insulin and tdTomato. A scan of a whole pancreas section, where multiple images are stitched together is shown (left upper panel) and high magnifications of an islet (middle panel). An example from an analysis is shown (right panels) where traced cells, INS+ cells and DAPI (for nuclei) are overlaid to allow for the percentage of INS+ islet cells which are traced to be determined..
C) Quantification of the number of HNF1b-labelled cells independent of islets and ducts in HNF1b-CreERT; tdTomato mice (n= 3 mice) at 1 week post-tamoxifen injection.
D) tdTomato IF in HNF1b-CreERT; tdTomato mice (n= 3 mice) at 1 week post-tamoxifen injection. Labelled cells independent of ducts and islets are circled with white dashed line.
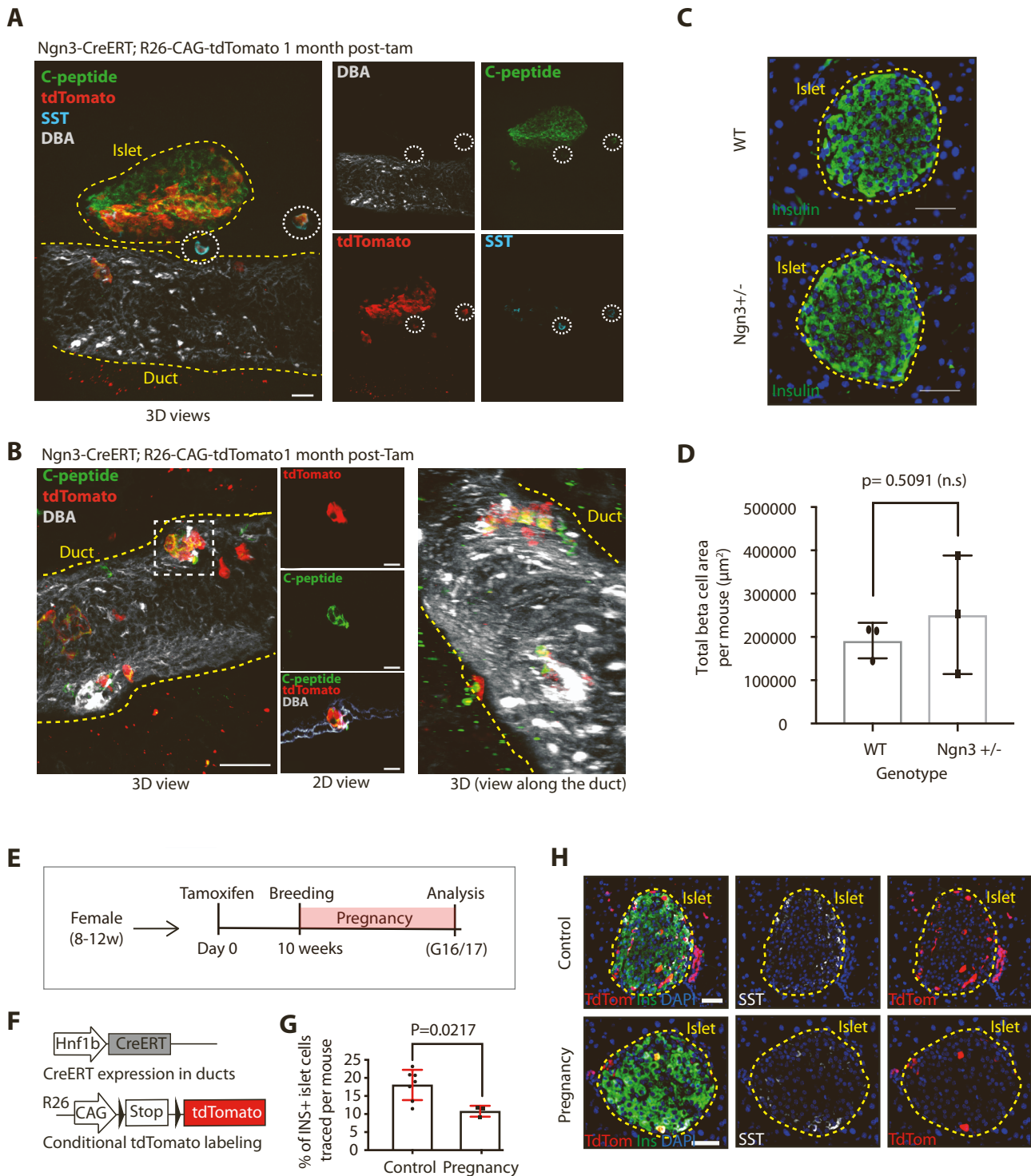
Figure S2: FLASH imaging of potentially migrating cells between duct and islet, related to Figure 2

A) 3D view following FLASH for tdTomato, C-peptide, tdTomato, SST and DBA of a pancreas from a Ngn3-CreERT; R26-CAG-tdTomato mouse at 1 month post-tamoxifen. Triple positive cells in between the duct and islet are circled. Scale bars, 20μm.

B) 3D view following FLASH for tdTomato, C-peptide, tdTomato and DBA of a pancreas from a Ngn3-CreERT; R26-CAG-tdTomato mouse at 1 month post-tamoxifen. Endocrine cell cluster within the duct is indicated by the white dash line. Scale bars, 20μm.

C) Immunofluorescence staining for Insulin in WT and Ngn3+/- mice pancreas. Scale bars, 50μm.

D) Quantification of the beta cell area in WT and Ngn3+/- mice pancreas. N=3 for WT and Ngn3+/-.

E) Schematic of experimental strategy to analyse the contribution of ductal cells to islets during pregnancy.

F) Schematic of the lineage tracing strategy.

G) Quantification of the percentage of INS+ islet cells traced per mouse in either mice at gestational day 16-17 of pregnancy or non-pregnant mice. Control N=7 mice, Pregnant N=3 mice.

H) Triple IF for Insulin (Ins), Somatostatin (Sst) and tdTomato (tdTom) in representative islets from control or pregnant mice. Scale bars, 50μm.
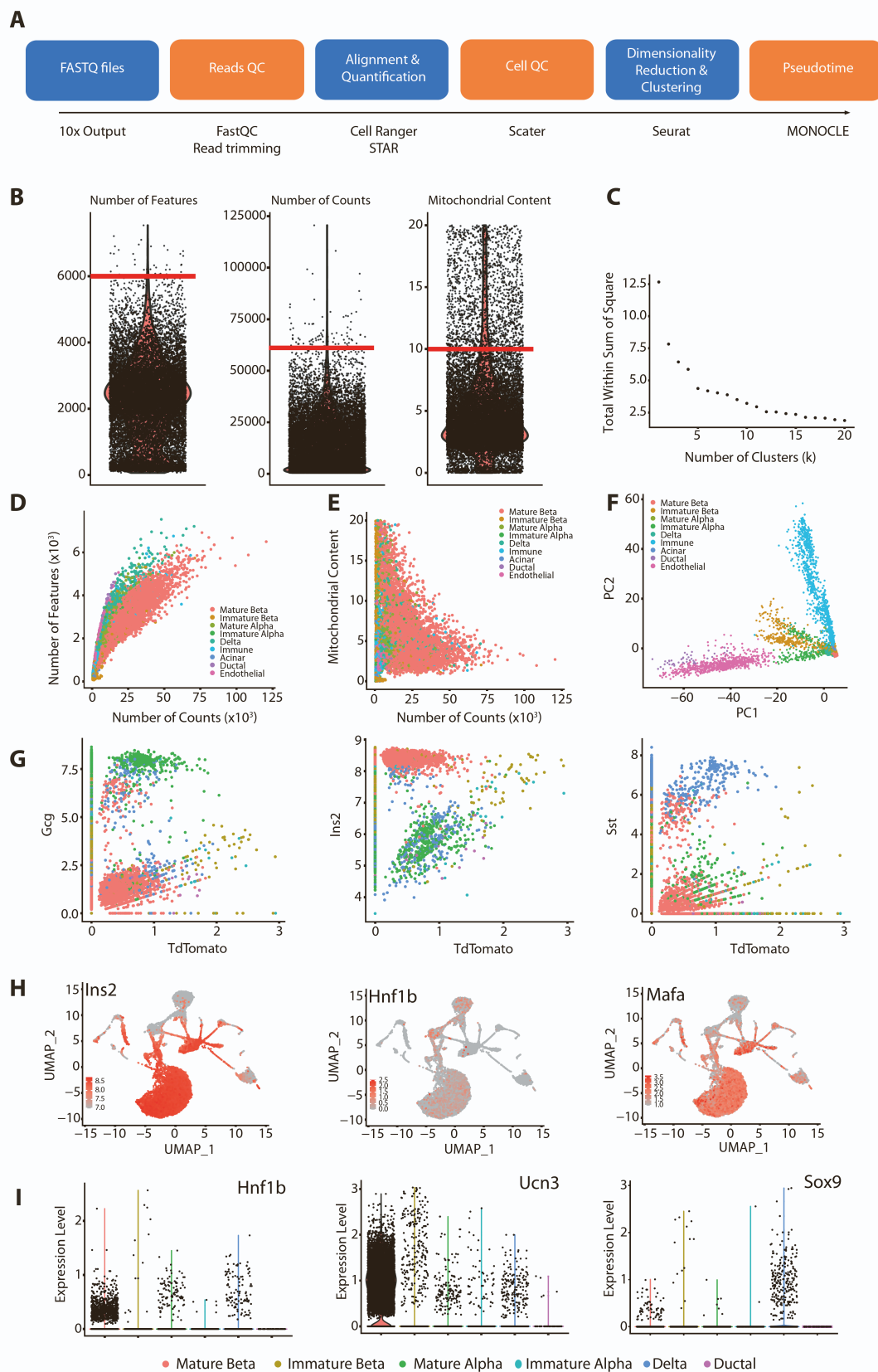
Figure S3: Analysis and validation of single-cell RNAseq data, related to Figure 4

A) Schematic of workflow for scRNAseq data analysis.
B) Cell quality control assessing number of features, count number and mitochondrial content. Red line indicate cutoff values.
C) Validation of unsupervised clustering by scree plot (k=10).
D) Number of detected features plotted against number of counts.
E) Mitochondrial content plotted against number of counts.
F) Principal component analysis of cells passing QC metrics.
G) Feature plots of traced cells against non-traced equivalents for Gcg, Ins2 and Sst expression.
H) UMAP plots of Ins2, Hnf1b and MafA across scRNAseq data set.
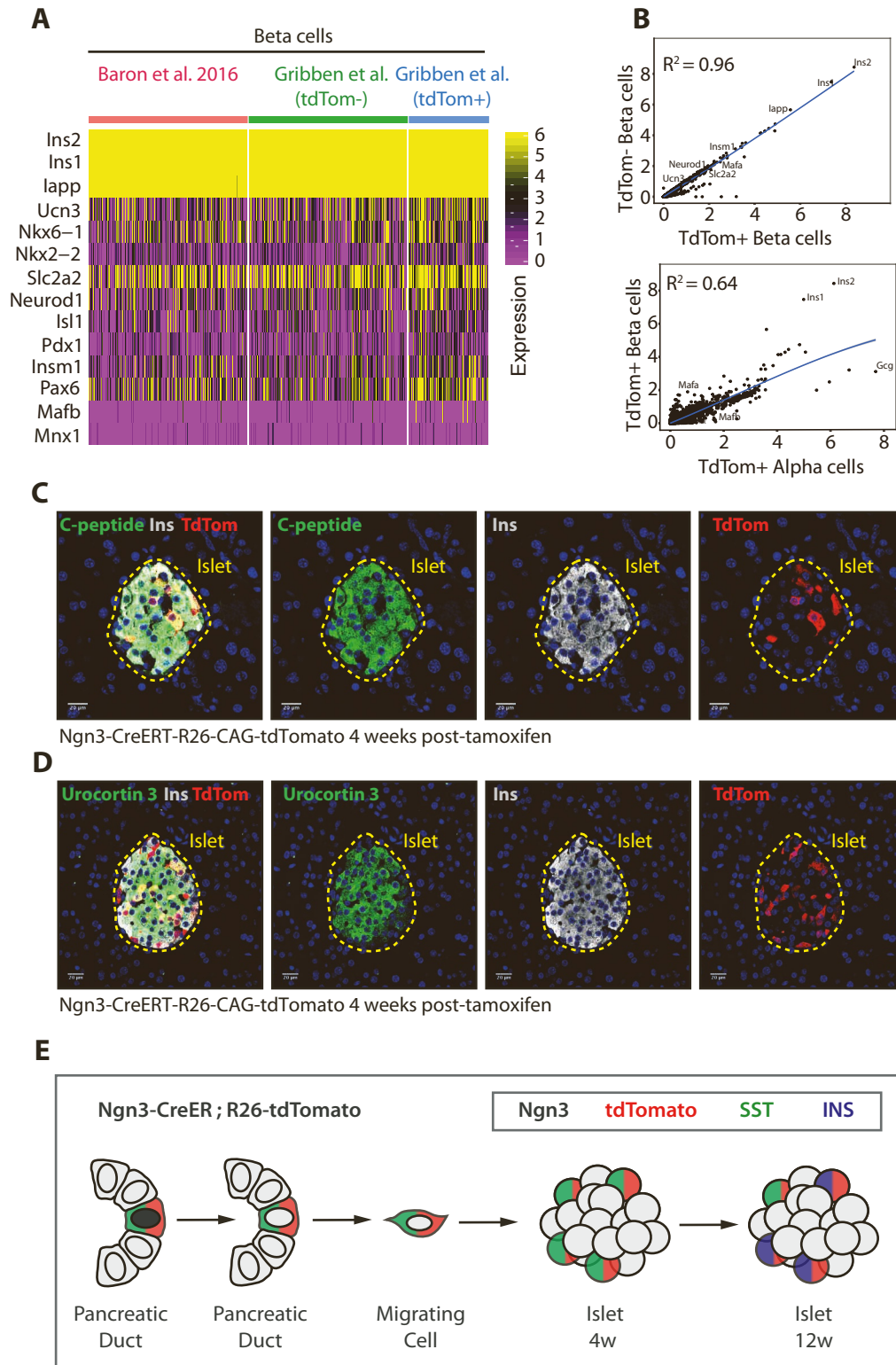I) Violin plots showing Hnf1b, Ucn3 and Sox9 expression per cluster

Figure S4: Analysis of tdTomato+ beta cells in Ngn3CreERT; R26-CAG-tdTomato mice, related to Figure 4.

(A)   Heatmap showing equivalent expression of beta cell markers across Baron dataset and non-traced and traced beta cells from our study.

(B)   Correlation analysis of tdTomato- and tdTomato+ (top) beta cells and tdTomato+ Alpha and tdTomato+ Beta cells

(C)   Triple IF for Insulin, C-peptide and tdTomato in Ngn3CreERT; R26-CAG-tdTomato mice at 4 weeks post-tamoxifen. A representative islet is shown.

(D)   Triple IF for Insulin, C-peptide and tdTomato in Ngn3CreERT; R26-CAG-tdTomato mice at 4 weeks post-tamoxifen. A representative islet is shown.

(E)   Proposed model for Ngn3+ ductal cell to beta cell differentiation.

Supplementary table 1

InsCreERT experiment

Time post-tamoxifen	Male/Female	Age when injected
1m	Male	20 weeks
1m	Male	26 weeks
1m	Female	17 weeks
1m	Female	17 weeks
6m	Male	21 weeks
6m	Female	10 weeks
6m	Male	18 weeks
6m	Male	18 weeks

Hnf1bCreERT experiment

Time post-tamoxifen	Male/Female	Age when injected
1 week	Male	12 weeks
1 week	Male	8 weeks
1 week	Male	8 weeks
1 week	Male	8 weeks
5 weeks	Male	16 weeks
5 weeks	Female	16 weeks
5 weeks	Male	16 weeks
5 weeks	Female	16 weeks
12 weeks	Male	10 weeks
12 weeks	Female	10 weeks
12 weeks	Female	8 weeks
12 weeks	Male	12 weeks
12 weeks	Female	10 weeks
12 weeks	Female	10 weeks

Ngn3CreERT experiment

Time post-tamoxifen	Male/Female	Age when injected
1 week	Male	43 weeks
1 week	Female	23 weeks
1 week	Female	22 weeks
4 weeks	Female	12 weeks
4 weeks	Female	16 weeks
4 weeks	Male	12 weeks

Ngn3CreERT experiment single cell RNAseq

Time post-tamoxifen	Male/Female	Age when injected
10 days	Female	10 weeks
10 days	Female	10 weeks
10 days	Male	12 weeks
10 days	Male	12 weeks
10 days	Female	12 weeks
10 days	Female	12 weeks

Ngn3CreERT Akita ducts quantification

Cohort	Male/Female	Age when injected
Akita tam injected	Male	13 weeks
Akita tam injected	Male	13 weeks
Akita tam injected	Female	34 weeks
WT	Male	43 weeks
WT	Female	23 weeks
WT	Female	22 weeks
Akita no tamoxifen control	Male	15 weeks
Akita no tamoxifen control	Male	15 weeks
Akita no tamoxifen control	Male	15 weeks
Akita no tamoxifen control	Male	15 weeks

Supplementary table 1. **Details of mice included in lineage tracing experiments, related to Figures 1-4.**

Supplementary table 2

Lineage tracing experiment	Average number of islet cells analysed per section
Hnf1bCreERT	1960
Ngn3CreERT	2130
InsCreERT	2854

Supplementary table 2. Details of the number of islets counted per lineage tracing experiment, related to Figures 1 and 2.